

# INTERNATIONAL SOCIETY FOR SOIL MECHANICS AND GEOTECHNICAL ENGINEERING



*This paper was downloaded from the Online Library of the International Society for Soil Mechanics and Geotechnical Engineering (ISSMGE). The library is available here:*

<https://www.issmge.org/publications/online-library>

*This is an open-access database that archives thousands of papers published under the Auspices of the ISSMGE and maintained by the Innovation and Development Committee of ISSMGE.*

*The paper was published in the proceedings of the 7<sup>th</sup> International Young Geotechnical Engineers Conference and was edited by Brendan Scott. The conference was held from April 29<sup>th</sup> to May 1<sup>st</sup> 2022 in Sydney, Australia.*

## The study of compacted soil behavior due to wetting under anisotropic condition through a series of simulations

L'étude du comportement des sols compactés en raison de mouillage dans des conditions anisotropiques à travers une série de simulations.

**Veerayut Komolvilas**

*Centre of Excellence in Geotechnical and Geoenvironmental Engineering, Department of Civil Engineering, Chulalongkorn University, Bangkok, Thailand, Veerayut.k@chula.ac.th*

**Chortham Srinil**

*Department of Civil Engineering, School of Engineering, King Mongkut's Institute of Technology Ladkrabang, Bangkok, Thailand*

**ABSTRACT:** This paper presents the wetting behavior of compacted soils under anisotropic condition through a series of simulations using the critical state model for unsaturated soils. Bishop's effective stress, the movement of state boundary surface due to the variation in the degree of saturation, and the soil water characteristic curves considering the effects of specific volume and hydraulic hysteresis are incorporated to generate the critical state model for unsaturated soils. Subloading surface concept is also applied to consider the effect of density. This model has been validated with the past experimental results. In the simulations, soil samples were isotropically compacted under the prescribed water contents on both dry and wet sides of optimum water content to generate the compacted soils at the degree of compaction of 90%, 95% and 100%. All compacted samples were subjected to a deviator stress and consecutively wet. Finally, the effects of compaction parameters including degree of compaction and water content along the compaction curve on the compacted soils behavior due to wetting under anisotropic condition were discussed.

**RÉSUMÉ :** Cet article présente le comportement de mouillage des sols compactés dans des conditions anisotropiques à travers une série de simulations utilisant le modèle d'état critique pour les sols non saturés. La contrainte effective de Bishop, le mouvement de la surface limite d'état dû à la variation du degré de saturation et la courbe caractéristique de l'eau du sol tenant compte des effets du volume spécifique et de l'hystérésis hydraulique sont incorporés pour générer le modèle d'état critique pour le sol non saturé. Le concept de surface de sous charge est également appliqué pour tenir compte de l'effet de la densité. Ce modèle a été validé avec les résultats expérimentaux antérieurs. Dans les simulations, les échantillons de sol ont été compactés de manière isotrope sous les teneurs en eau prescrites sur les côtés sec et humide de la teneur en eau optimale afin de générer le sol compacté au degré de compactage de 90 %, 95 % et 100 %. Tous les échantillons compactés ont été soumis à une contrainte de déviation et successivement humides. Enfin, les effets des paramètres de compactage, y compris le degré de compactage et la teneur en eau le long de la courbe de compactage, sur le comportement du sol compacté dû au mouillage dans des conditions anisotropes ont été discutés.

**KEYWORDS:** compaction; wetting; anisotropic condition; critical state model; unsaturated soil.

### 1 INTRODUCTION

In compaction work, engineers usually use the compaction curve to control the compaction quality. The typical compaction curve is the convex-upward curve which there is an optimum water content at the maximum dry density. Since the maximum dry density in compaction is hardly achieved in practice, therefore allowable compaction specifications were typically set. In engineering standard requirement (e.g., FP-14, NAVFAC DM7-02), dry density of compacted soil shall be achieved degree of compaction of 90% to 95%. Compaction water content shall not be deviated from the optimum water content in the range of about  $\pm 2\%$ . However, several failures of the compacted soil against the wetting phenomena have occurred (Miller et al. 2001, Oh & Lu 2015, Subramanian et al. 2017). One of the reasons is the characteristics of the soils compacted on the dry side and the wet side of optimum water content are significantly different even at the same dry density (Lambe 1958). For instance, the shear strength of compacted soil decreases with the increase of compaction water content (Turnbull & Foster 1956, Seed & Chan 1961, Yoder & Witezak 1975, Han & Vanapalli 2016), while the shear strength of soil compacted on the dry side of optimum water content significantly reduces after wetting (Yoder & Witezak 1975, Rollings & Rollings 1996). In addition, the soils compacted on the dry side of optimum water content and low

degree of compaction result in the increasing of wetting induced collapse under anisotropic condition (Yoder & Witezak 1975, Lawton et al. 1989, Lawton et al. 1992). Therefore, compaction specifications for the soil structures against wetting phenomena should consider the effects of water content and degree of compaction on the compacted soil behaviors.

Many researchers have studied soil compaction through both experiments and simulations to develop the constitutive models for the compaction of unsaturated soils (Sun et al. 2007a, Tarantino & De Col 2008, Kikumoto et al. 2010, Alonso et al. 2013, Srinil et al. 2019). In addition, the strengths and the failures of unsaturated soils under the long-term shearing and the wetting induced collapse (Sivakumar & Wheeler 2000, Wheeler & Sivakumar 2000, Gallipoli et al. 2003, Sun et al. 2007b, Sivakumar et al. 2010, Zhou & Sheng 2015) have also been studied through the combination of experiments and simulations. However, the effects of compaction water content and degree of compaction on the behaviors of wetting induced collapse under anisotropic condition of compacted soil have not been widely studied yet, especially in the framework of the simulation.

This paper presents the constitutive model for unsaturated soils (Komolvilas & Kikumoto 2017, Srinil et al. 2019) that could predict the compaction mechanism and wetting induced collapse under anisotropic condition. The model incorporates Bishop's effective stress, the movement of state boundary surface

due to the variation in the degree of saturation, and the soil water characteristic curves considering the effects of specific volume and hydraulic hysteresis are incorporated to generate the critical state model for unsaturated soils. Subloading surface concept is also applied to consider the effect of density. In the simulations, typical convex-upward compaction curve was numerically generated by the model. The compacted soils at the degree of compaction of 90%, 95% and 100% were sheared and consecutively wet to the fully saturated condition. Finally, the effects of water content and degree of compaction on the mechanism of wetting induced collapse under anisotropic condition of compacted soils were discussed.

## 2 BASIC CONCEPT OF THE MODEL

### 2.1 Constitutive model for unsaturated soils

A series of simulations in this paper was simulated by a critical state model for unsaturated soils (Komolovilas & Kikumoto 2017, Srinil et al. 2019). Basic concepts of the model are described in this section and summarized in Figure 1.

First, Bishop's effective stress ( $\sigma''$ ) (Bishop 1959) is used to formulate the model. Regarding the experimental evidence, we assume that Bishop's effective stress parameter follows the variation of degree of saturation for simplicity (Schrefler 1984). Therefore,  $\sigma''$  can be written as shown in Eq. 1.

$$\sigma'' = \sigma - (1 - S_r)u_a \mathbf{1} - S_r u_w \mathbf{1} \quad (1)$$

Second, soil water characteristic curves (SWCCs) which is generally described as the relation between suction and the degree of saturation are incorporated for predicting the hydraulic behavior of unsaturated soils. In this model, we extend the SWCC model (See Eq. 2) from a classical SWCC model (Genuchten 1980)

$$\frac{S_r^A - S_{rmin}}{S_{rmax} - S_{rmin}} = S_e^A(s^*) = \left\{1 + (\alpha^A s^*)^n\right\}^{-m} \quad A = d, w \quad (2)$$

where modified suction ( $s^*$ ) (See Eq. 3) and ratio  $I_h$  (See Eq. 4) are applied to consider effects of density and hysteresis, respectively.

$$s^* = s \left( \frac{v-1}{v_{ref}-1} \right)^{\xi_e} \quad (3)$$

$$I_h = \frac{S_r - S_r^w}{S_r^d - S_r^w} \quad (4)$$

Third, we initially formulate the critical state model based on the modified Cam-clay (Roscoe & Burland 1968) to describe the behavior of saturated, normally consolidated (NC) soils. We assume that the specific volume ( $v$ ) of saturated NC soils (loosest specific volume) is uniquely defined in the space of mean effective stress ( $p''$ ) and stress ratio ( $\eta'' = q/p''$ ). To extend the model for capturing the behavior of unsaturated soils, we assume that the specific volume of unsaturated NC soils increases by linear relationship of  $\Psi(S_r)$  with decreasing the degree of saturation for simplicity as written by Eq. 5.

$$\Psi = \psi(1 - S_r) \quad (5)$$

This is because the unsaturated soils show a relatively high stiffness and retains a larger specific volume than the saturated soils. Therefore, with the assumption of associated flow rule, the yield function ( $f$ ) for unsaturated soils is given by Eq. 6 considering the movement of the state boundary surface (SBS).

$$f = (\lambda - \kappa) \ln \frac{p'' \left\{1 + \left(\frac{\eta''}{M}\right)^2\right\}}{p_0' \left\{1 + \left(\frac{\eta_0'}{M}\right)^2\right\}} - v_0 \varepsilon_p^p + (\Psi - \Psi_0) - (\Omega - \Omega_0) \quad (6)$$

Last, the model considers the effect of density on the stress-strain characteristic by subloading surface concept (Hashiguchi & Ueno 1977) to govern the behavior of overconsolidated soils. This is because, soils exhibit elastoplastic deformation even in an overconsolidated state and then gradually approach the normal consolidation plane with the increase in the stress level. The difference  $\Omega$  between the specific volume on the SBS and the current specific volume under the current mean effective stress, deviator stress, and degree of saturation is applied as a measure of density (Kikumoto et al. 2010) as shown in Eq. 7.

$$\dot{\Omega} = -\omega \Omega |\Omega| v_0 \|\dot{\varepsilon}^p\| \quad (7)$$

### 2.2 Drainage conditions

Drainage conditions of air pressure and water pressure are applied for simulating compaction, fully drained shearing and wetting of unsaturated soils.

Compaction is the densification process by exhaustion of air void and keeping water content constant, therefore exhausted-air and undrained-water conditions are controlled by  $u_a = 0$  and  $\dot{w} = 0$ , respectively, in the simulation.

Fully drained shearing is controlled by  $u_a = 0$  and  $u_w = 0$  in the simulation for exhausted air and drained water conditions, respectively.

Wetting process is the condition that air is able to drain out of the soils and the total stress does not change but water is able to increase or decrease during the test. This condition is simulated by keeping  $u_a = 0$  and  $\dot{\sigma} = 0$ , and applying  $u_w (> 0)$  to decrease suction for wetting.

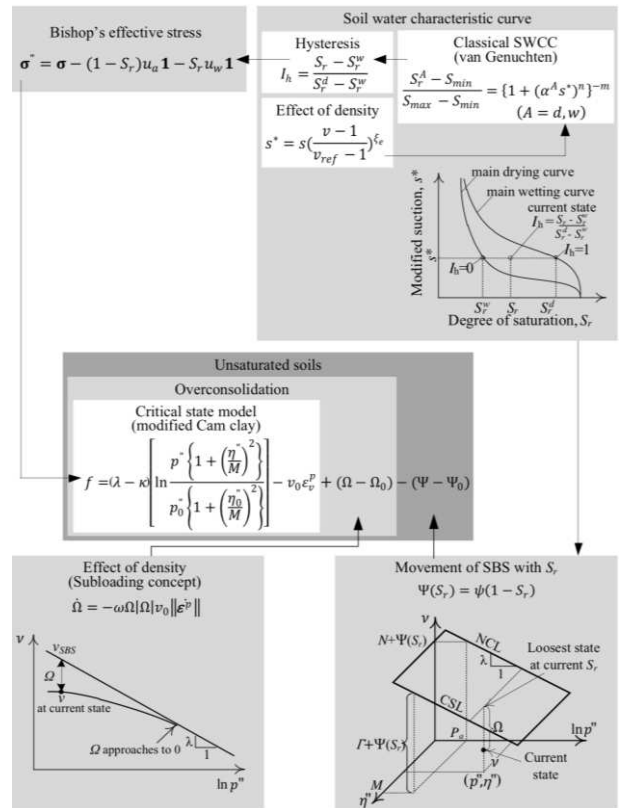


Figure 1. Basic concepts of the constitutive model for unsaturated soils.

### 3 MODEL VALIDATIONS

To simulate the mechanisms of unsaturated soils, including soil compaction, fully drained shearing and wetting induced collapse under anisotropic condition, the constitutive model of unsaturated soils has been validated through the laboratory experiments explained below using the calibrated constitutive model parameters as summarized in Table 1 and Table 2.

#### 3.1 Mechanism of static compaction

One-dimensional (1-D) static compaction tests on 5:5 mixed Toyoura sand and Fujinomori clay by weight (hereafter referred to as “mixed clay-sand”) were conducted to validate the model for compaction simulation. Standard oedometer testing apparatus was used with water-impermeable plastic sheets to apply exhausted-air, undrained-water condition for compaction. The specific gravity ( $G_s$ ) was 2.673. The initial void ratio ( $e_0$ ) of the prepared specimens were about 1.14. Water content ( $w$ ) were in the range of 6% to 19% which were on the dry side of optimum water content ( $w_{opt}$ ). Applied vertical compaction stresses ( $\sigma_v$ ) were 19.6, 314.0 and 1256.0 kPa, respectively. By the constitutive model, the simulation processes and the initial state of soils were similarly set as described in the experiments. In addition, the compaction water contents were extended to predict the compaction curve on the wet side of optimum water content. The calibrated constitutive model parameters of mixed clay-sand (See Table 1 and Table 2) were used in the simulations.

Table 1. Model parameters for stress-strain characteristics.

Parameters	Mixed clay-sand	Pearl clay	Descriptions
$\lambda$	0.12	0.10	Compression index
$\kappa$	0.01	0.001	Swelling index
$M$	1.3	1.1	Critical state stress ratio
$\nu_e$	0.25	0.20	Poisson's ratio
$N$	1.78	2.2	Reference specific volume
$\omega$	100.0	100.0	Effect of density
$\psi$	0.35	0.60	Effect of $S_r$ on the position of SBSs

Table 2. Soil water characteristic curve parameters

Parameters	Mixed clay-sand	Pearl clay	Descriptions
$S_{max}$	1.0	1.0	Maximum $S_r$
$S_{min}$	0.1	0.1	Minimum $S_r$
$\alpha_d$ (1/kPa)	0.01	0.03	Parameter for main drying curve
$\alpha_w$ (1/kPa)	0.60	0.10	Parameter for main wetting curve
$n$	2.0	1.5	Parameters for the shape of main curves
$m$	0.5	0.1	
$\xi_h$	100.0	100.0	Effect of hysteresis
$\xi_e$	5.0	14.0	Effect of void ratio

Compression behaviors, variation of degree of saturation due to compaction, and compaction curves obtained from the experiments and simulations are compared in Figures 2, 3 and 4, respectively. We can see that the model could predict the experimental data well. In particular, the model could generate the typical convex-upward compaction curves with maximum dry densities and optimum water content. Moreover, the translation of the compaction curve to the upper left (or lower water content and higher dry density) due to the increasing of compaction effort is also observed.

#### 3.2 Mechanism of wetting under anisotropic condition

Wetting tests under anisotropic stress condition on Pearl clay with different stress state and density (Sun et al. 2007b) are used to validate the model capturing wetting induced collapse behavior under anisotropic condition of unsaturated soils. The initial void ratios of the prepared specimens were 1.15 and 1.42 as the representative of dense soil and loose soil, respectively. First, the specimens were sheared under the fully drained condition at the mean stress constant. Afterwards, the wetting process was performed by decreasing suction to 0 kPa (fully saturated condition) at the constant deviatoric stress. Finally, shearing process was reapplied. Using the proposed constitutive model, the simulation processes and the initial states of soil were similarly set as described in the experiments. The calibrated constitutive model parameters of Pearl clay (See Table 1 and Table 2) were used in the simulations. Volumetric and deviatoric deformations due to wetting under anisotropic condition observed in the experiments (Sun et al. 2007b) and the simulations are compared in Figure 5. We found that the model could appropriately predict the experiment results considering the effects of the stress state and density on fully drained monotonic shearing and wetting collapse behaviors.

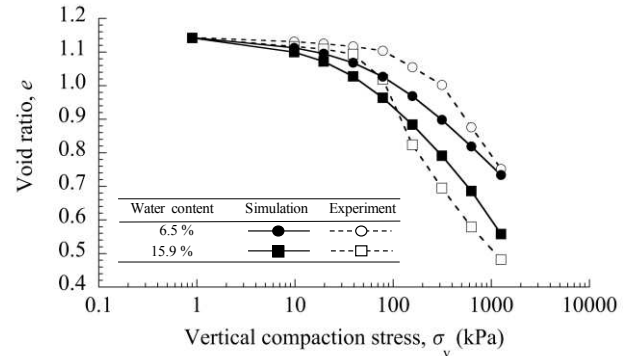


Figure 2. Model validation of compression behavior under exhausted air and undrained water conditions in the relation of  $\sigma_v$  and  $e$ .

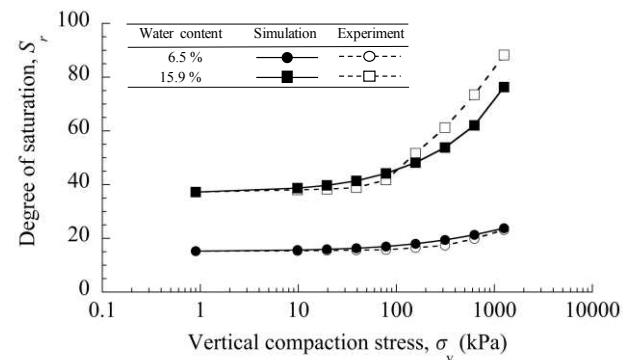


Figure 3. Model validation of compression behavior under exhausted air and undrained water conditions in the relation of  $\sigma_v$  and  $S_r$ .



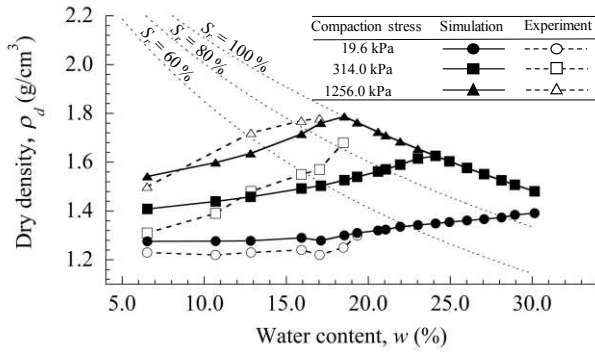


Figure 4. Model validation of compaction curve simulation

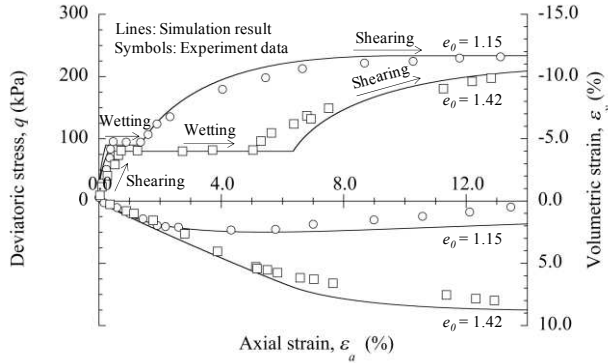


Figure 5. Model validation of wetting induced collapse under anisotropic condition of Pearl clay.

#### 4 A SERIES OF SIMULATIONS

In a series of simulations, soil compaction simulation was firstly performed to produce compacted soils following by simulation of wetting under anisotropic condition. This aims to investigate the wetting induced collapse under anisotropic condition of compacted soils considering the effect of compaction water content and degree of compaction. The calibrated constitutive model parameters of mixed clay-sand (Table 1 and Table 2) were used in a series of simulations.

##### 4.1 Soil compaction

The initial state of soil specimens were set as followings; void ratio of 0.95; water content of 6.37 %; degree of saturation of 17.94 %; mean net stress of 20.0 kPa; pore air pressure of 98.0 kPa; and pore water pressure of 62.50 kPa. Then, the initial water content was increased to the prescribed water contents along the compaction curve by decrease of suction (increase of pore water pressure) under constant mean net stress. Afterwards, the prepared specimens were isotopically compressed to the compaction stress of 1256.0 kPa and consecutively unloaded to the initial mean net stress of 20.0 kPa under exhausted air and undrained water conditions. Finally, the compaction curve was plotted as shown in Figure 6. From the simulation results, the model could demonstrate the typical convex-upward curve with maximum dry density and optimum water content which is firstly published by Proctor (1933).

##### 4.2 Wetting under anisotropic condition of compacted soils

In this paper, we selected the following compacted specimens from the simulated compaction curve (Figure 6) to investigate the wetting induced collapse under anisotropic condition; the maximum dry density at the optimum water content (O100); 95% of maximum dry density on dry side (D95) and wet side (W95)

of optimum water content; and 90% of maximum dry density on dry side (D90) and wet side (W90) of optimum water content.

Figure 7 illustrates the simulation procedure of wetting induced collapse under anisotropic condition. First, all selected specimens were sheared to the deviatoric stress of 50 kPa under mean net stress constant and fully drained condition by using stress—controlled. Then, they were wet by decreasing suction to 0 kPa (fully saturated condition) at the constant deviatoric stress. The simulation results of wetting under anisotropic condition on compacted specimens at the specified degree of compactions are shown in Figure 8. The deviatoric strain induced by shearing process and wetting process of each compacted specimen in Figure 8 could be illustrated in Figure 9.

In Figure 9, from the simulation results, we could sort the stiffness of compacted soil under the shearing process (black bar chart in Figure 9) from greatest to least as follows: D90 > D95 > O100 > W95 > W90. It reveals that, at a given compaction effort in a compaction curve, the shear strengths decrease with the increase of water content. This simulation result corresponds

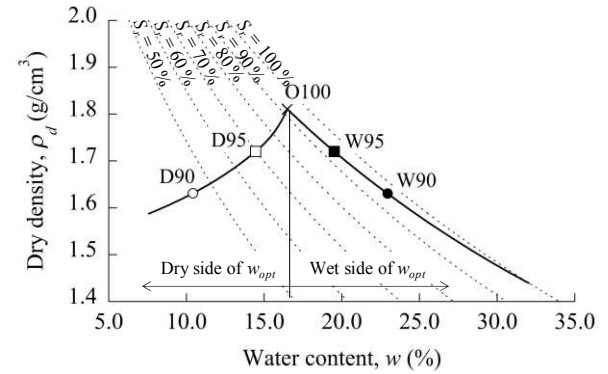


Figure 6. Simulation result of compaction curve.

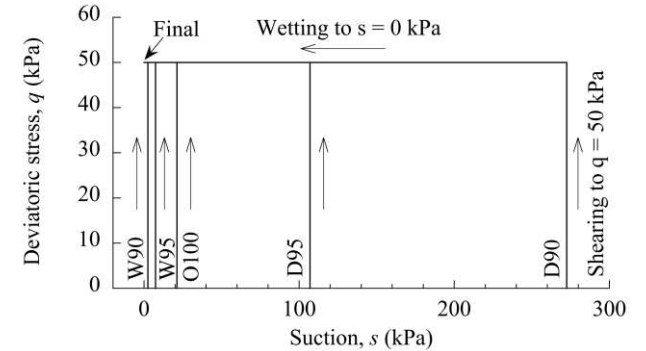


Figure 7. Simulation procedures of wetting under anisotropic condition on compacted specimens at the specified degree of compactions.

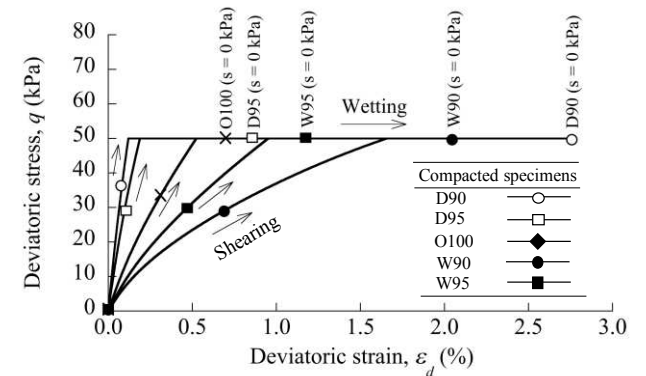


Figure 8. Simulation results of wetting under anisotropic condition on compacted specimens at the specified degree of compactions.

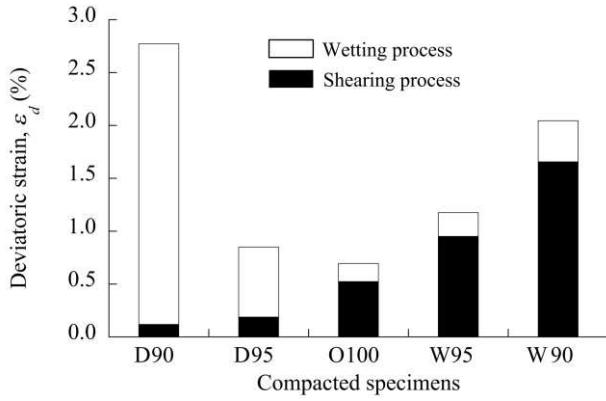


Figure 9. Deviatoric strain induced by wetting under anisotropic condition of compacted specimens at the fully saturated conditions

with the previous experimental evidence of many researchers (Turnbull & Foster 1956, Seed & Chan 1961, Yoder & Witezak 1975, Han & Vanapalli 2016). However, the largest magnitude of deviatoric strain under the wetting process (white bar chart in Figure 9) is observed on the soil compacted on the dry side of optimum. Then it is followed by the soils compacted on wet side of optimum and at optimum water content, respectively. Since wetting induced deviatoric strain of the soil compacted on the dry side of optimum is extremely high, therefore we can state that the water content dominantly affects the wetting collapse under anisotropic condition. Moreover, low degree of compaction causes large wetting induced deviatoric strain is observed on both wet side and dry side of optimum water content. The simulation results conform with the experimental evidence that wetting the loose soil results in larger wetting induced deviatoric strain than the dense soil (Sun et al. 2007b).

Considering both shearing and wetting induced deviatoric strain of the compacted soils, the minimum deviatoric strain is at the optimum water content as shown in Figure 9. We can state that shear resistance of soil compacted at the optimum water content (O100) is the optimum point for the soil structure against wetting induced collapse under anisotropic condition. In the case that the optimum water content could not be reached, shear resistance of soils compacted with high degree of compaction is better than low degree of compaction on each side of compaction as shown in Figure 9. At degree of compaction of 95%, the shear resistance of soil compacted on the dry side of optimum (D95) is slightly higher than that of the wet side of optimum (W95). However, it shows inverse tendency at lower degree of compaction, which soil compacted on the wet side of optimum (W90) is significantly better than dry side of optimum (D90).

## 5 CONCLUSIONS

The behavior of compacted soils due to wetting under anisotropic condition has been investigated through a series of simulations using the critical state model for unsaturated soils. The model incorporates Bishop's effective stress, the movement of state boundary surface due to the variation in the degree of saturation, and the soil water characteristic curves considering the effects of specific volume and hydraulic hysteresis are incorporated to generate the critical state model for unsaturated soils. Subloading surface concept is also applied to consider the effect of density. The model has been validated through the past experimental results of the static compaction tests and the wetting tests under anisotropic condition. In the simulations, the typical convex-upward compaction curve was numerically generated by the model. Then, the compacted soils at the degree of compaction of 90%, 95% and 100% on both wet and dry sides of optimum water content were sheared and consecutively wet to

the fully saturated condition. Some key conclusions from this study can be summarized as following:

- The proposed model can predict the wetting-induced deformation of compacted soils under anisotropic condition.
- Regarding the wetting process under anisotropic condition, water content shows the predominant factor of wetting-induced deformation. The shear resistance of soil compacted on the wet side is higher than that of the dry side on any degree of compaction.
- The shear resistance of compacted soils subjected to shearing and wetting under anisotropic condition shows the convex-downward shape as shown in Figure 9, which the minimum deviatoric strain is at the optimum water content. The soils that compacted under higher degree of compaction show higher shear resistance. At higher degree of compaction, the shear resistance of soils compacted on the dry side of optimum is slightly higher than that of the wet side of optimum. However, it shows inverse tendency at lower degree of compaction, which the shear resistance of soils compacted on the wet side of optimum is significantly better than dry side of optimum.

Therefore, the findings in this paper should be considered in the compaction requirements for the soil structures against the wetting phenomena to alleviate the unexpected wetting-induced deformation.

## 6 NOTATIONS

The following symbols are used in this paper.

bold letters	vectors and tensors
$\  \quad \ $	the norm of tensor
$\dot{\quad}$	the time derivative of a variable
$  \quad  $	the absolute value of a variable
$e$	void ratio
$f$	yield function
$G_s$	specific gravity
$P_a$	atmospheric pressure
$p_{net}$	mean net stress
$p''$	mean effective stress
$q$	deviator stress
$S_{max}, S_{min}$	maximum and minimum $S_r$
$S_r$	degree of saturation
$s, s^*$	suction and modified suction
subscript $v, d$	volumetric and deviatoric components
subscript $v, a$	vertical and axial directions
subscript 0	initial value
superscript $d, w$	main drying and wetting curves
superscript $p$	plastic component
$u_a, u_w$	pore air and pore water pressures
$v$	specific volume ( $= 1 + e$ )
$\nu_e$	Poisson's ratio
$\nu_{ref}, \xi_e$	material parameters for modified suction (reference specific volume and effect of density);
$\nu_{SBS}$	specific volume on the SBS
$w$	water content
$w_{opt}$	optimum water content
$\alpha, m, n$	material parameters of van Genuchten's equation for soil water characteristic curve
$\varepsilon$	strain in a specified direction
$\boldsymbol{\varepsilon}$	strain tensor
$\eta''$	Bishop's effective stress ratio
$\kappa$	swelling index

$\lambda$	compression index
$M$	critical state stress ratio
$N, \Gamma$	reference $v$ on the SBS of a saturated soil under $P_a$ at isotropic stress and at critical state stress ratio
$\xi_h$	material parameter for the rate of evolution of $I_h$
$\rho_d$	dry density
$\sigma$	total stress in a specified direction
$\boldsymbol{\sigma}$	Cauchy's total stress tensor
$\boldsymbol{\sigma}'$	Bishop's effective stress tensor
$\Psi$	state parameter of $S_r$ that satisfies 0 at saturated state ( $S_r = 1$ )
$\psi$	material parameter representing the volumetric distance of SBSs for fully-dried and fully-saturated states in the volumetric direction
$\Omega$	difference between the current specific volume and the specific volume on the SBS under the current $p'', q$ , and $S_r$
$\omega$	parameter controlling rate of evolution of $\Omega$ for effect of density
$\mathbf{I}$	the second-order identity tensor $\left( \delta_{ij} = \begin{cases} 1 & (i = j) \\ 0 & (i \neq j) \end{cases} \right)$

## 7 ACKNOWLEDGEMENTS

This work was financially supported by Office of the Permanent Secretary, Ministry of Higher Education, Science, Research and Innovation: Grant No. RGNS 63-019. The authors would like to thank Mentors (Associated professor Mamoru Kikumoto and Professor Suched Likitlersuang) for guidance and useful advice. Authors would like to thank for the 1-D static compaction testing result conducted by Ms. Koike Mana for her master graduation in graduate school of Nagoya Institute of Technology under the supervision of Professor Teruo Nakai and Associated professor Mamoru Kikumoto.

## 8 REFERENCES

- Alonso E., Pinyol N.M. and Gens A. 2013. Compacted soil behaviour: initial state, structure and constitutive modelling. *Géotechnique* 63(6), 463–478.
- Bishop A.W. 1959. The principal of effective stress. *Teknisk Ukeblad* 106(39): 859–863.
- Federal Highway Administration 2014. *Standard Specifications for Construction of Roads and Bridges on Federal Highway Projects FP-14*, Section 204. Washington, D.C.
- Gallipoli D., Wheeler S.J. and Karstunen M. 2003. Modelling the variation of degree of saturation in a deformable unsaturated soil. *Géotechnique* 53(1), 105–112.
- Genuchten V. 1980. A closed-form equation for predicting the hydraulic conductivity of unsaturated soils. *Soil Science Society of America Journal* 44(5), 892–898.
- Han Z. and Vanapalli S.K. 2016. Stiffness and shear strength of unsaturated soils in relation to soil - water characteristic curve. *Géotechnique* 66(8), 627–647.
- Hashiguchi K. and Ueno M. 1977. Elastoplastic constitutive laws of granular material. *Proceeding of the 9th International Conference on Soil Mechanics and Foundation Engineering*, 73–82.
- Kikumoto M., Kyokawa H., Nakai T. and Shahin H.M. 2010. A simple elasto-plastic model for unsaturated soils and interpretations of collapse and compaction behaviours. In E. Alonso, & A. Gens (Ed.), *Proceeding of 5th International Conference on Unsaturated Soils*, Barcelona, 849–855.
- Komolvilas V. and Kikumoto M. 2017. Simulation of liquefaction of unsaturated soil using critical state soil model. *International Journal for Numerical and Analytical Methods in Geomechanics* 41, 1217–1246.
- Lambe T.W. 1958. The structure of compacted clay. *Journal of the Soil Mechanics and Foundations Division* 84(2), 1–1655–34.
- Lawton E.C., Fragaszy R.J. and Hetherington M.D. 1992. Review of wetting-induced collapse in compacted soil. *Journal of Geotechnical Engineer* 118(9), 1376–1394.
- Lawton E.C., Fragaszy R.J. and Hardcastle J.H. 1989. Collapse of compacted clayey sand. *Journal of Geotechnical Engineering* 115(9), 1252–1267.
- Miller G.A., Muraleetharan K.K. and Lim Y.Y. 2001. Wetting-Induced Settlement of Compacted-Fill Embankments. *Transportation Research Record* 1755(1), 111–118.
- NAVFAC 1986. *Foundations & Earth Structures DM 7.02*, Alexandria, Virginia.
- Oh S. and Lu N. 2015. Slope stability analysis under unsaturated conditions: Case studies of rainfall-induced failure of cut slopes. *Engineering Geology* 184, 96–103.
- Proctor R.R. 1933. *Fundamental principles of soil compaction*. Engineering News-Record 111(9), 286–289.
- Rollings M.P. and Rollings R.S. 1996. *Geotechnical Materials in Construction*. New York: McGraw-Hill.
- Roscoe K.H. and Burland J.B. 1968. On the generalized stress-strain behaviour of wet clay. *Engineering plasticity*, 535–609.
- Schrefler B.A. 1984. The finite element method in soil consolidation (with applications to surface subsidence). *Ph. D. Thesis*. University Collage of Swansea.
- Seed H.B. and Chan C.K. 1961. Compacted clays: a symposium: structure and strength characteristics. *Transactions of the American Society of Civil Engineers* 126(1), 1344–1384.
- Sivakumar V. and Wheeler S.J. 2000. Influence of compaction procedure on the mechanical behaviour of an unsaturated compacted clay. Part 1: Wetting and isotropic compression. *Géotechnique* 50(4), 359–368.
- Sivakumar V., Sivakumar R., Murray E.J., Mackinnon P. and Boyd J. 2010. Mechanical behaviour of unsaturated kaolin (with isotropic and anisotropic stress history). Part 1: Wetting and compression behaviour. *Géotechnique* 60(8), 581–594.
- Srinil C., Kikumoto M. and Komolvilas V. 2019. Simulation on liquefaction of unsaturated compacted soils - effect of compaction degree. *Proceedings of the 7th International Conference on Earthquake Geotechnical Engineering*, Rome, Italy, 5095–5103.
- Subramanian S.S., Isikawa T. and Tokoro T. 2017. Stability assessment approach for soil slopes in seasonal cold regions. *Engineering Geology* 221, 154–169.
- Sun D.A., Cui H.B., Matsuoka H. and Sheng D.C. 2007a. A three-dimensional elastoplastic model for unsaturated compacted soils with hydraulic hysteresis. *Soils and Foundations* 47(2), 253–264.
- Sun D.A., Sheng D.C. and Xu Y. 2007b. Collapse behaviour of unsaturated compacted soil with different initial densities. *Canadian Geotechnical Journal* 44, 673–686.
- Tarantino A. and De Col E. 2008. Compaction behaviour of clay. *Géotechnique* 58 (3), 199–213.
- Turnbull W.J. and Foster C.R. 1956. Stabilization of Materials by Compaction. *Journal of the Soil Mechanics and Foundation Division* 82(2), 1–23.
- Wheeler S.J. and Sivakumar V. 2000. Influence of compaction procedure on the mechanical behaviour of an unsaturated compacted clay. Part 2: shearing and constitutive modelling. *Géotechnique* 50(4), 369–376.
- Yoder E.J. and Witczak M.W. 1975. *Principles of pavement design*. 2nd Edition. New York: John Wiley and Sons.
- Zhou A. and Sheng D. 2015. An advanced hydro-mechanical constitutive model for unsaturated soils with different initial densities. *Computers and Geotechnics* 63, 46–66.